Available online at www.sciencedirect.com
ScienceDirect
Journal of Colloid and Interface Science 301 (2006) 554–559
JOURNAL OF Colloid and Interface Science
www.elsevier.com/locate/jcis

Effect of sulfate on the surface and catalytic properties of iron–chromium mixed oxide pillared clay

T. Mishra [a,*], K.M. Parida [b]

[a] *ACC Division, National Metallurgical Laboratory, Jamshedpur 831007, Jharkhand, India*
[b] *BP&EM Department, Regional Research Laboratory, Bhubaneswar, Orissa, India*

Received 3 March 2006; accepted 4 May 2006

Available online 12 June 2006

Abstract

Sulfate-supported iron–chromium mixed oxide pillared clay was prepared varying the sulfate loading from 1 to 5 wt% by the incipient wetness method and characterized by low-angle XRD, BET surface area, and ammonia TPD. All the samples were found to be stable up to 500 °C having the basal spacing $\geqslant$17.7 Å even after sulfate impregnation. Formation of strong Lewis acid sites and decrease in the number of Brønsted acid sites due to the sulfate loading were observed from the ammonia TPD curve. Catalytic properties of the sulfated materials were evaluated with the help of methanol conversion and aromatic alkylation reactions and correlated with the surface area and TPD results. For methanol conversion, decomposition product selectivity increases due to the sulfate addition. A negligible decrease in the surface area and a substantial increase in the catalytic activity were observed due to the sulfate loading of 1–2 wt%. However, a significant decrease in the surface area as well as catalytic activity was observed for the 3 wt% and above sulfate loaded samples which may be due to the partial blockage of pores by excess sulfate. Results shows the importance of acidity of the material due to sulfate loading (up to 2 wt%) and thus can be used as a better acid catalyst.

Keywords: Sulfated; Iron–chromium mixed oxide pillared clay; Methanol; Alkylation

1. Introduction

Insertion of metal oxide pillars into the interlayer region of the smectite group of clays lead to the development of a new class of thermally stable solids having micropores larger than those in zeolites [1]. In particular, insertion of transition metal oxide pillars received much interest as pillars are themselves catalytically active for a number of reactions [2,3]. In this context, several attempts to introduce mixed oxide pillars by different methods were also reported. However, most of these involve oxide species such as CrO_x, FeO_x, GaO_x, or rare earth metal oxide with aluminum oxide [4–7]. In particular, reports on mixed oxide transition metal pillared clays are still limited [8,9]. In certain cases it was observed that the mixed oxide pillared materials exhibit enhanced surface area and also surface acidity in comparison with single oxide pillared materials. Similarly, in our earlier report on iron–chromium mixed oxide pillared clay, higher basal spacing and better catalytic activity were noted [9].

Recently, anion-supported pillared clay also attracted the attention of number of researchers due to the enhancement of acidity and catalytic activity [10–14] similar to that of sulfated metal oxides. As far as catalytic activity is concerned the regular pore size of pillared clay has the advantage over the simple metal oxide systems. However, decreasing surface area and thermal stability of the pillared material due to sulfate impregnation were the main bottleneck problems [11]. In this context sulfate incorporation from the precursor solution was suggested to be beneficial [14]. Therefore, there is still a need for a detailed investigation on the effect of anion loading on the textural and catalytic activity of the pillared material. On the other hand, it was also reported that sulfated iron oxide [15] can behave as a superacid similar to that of sulfated zirconia and titania. However, most of the reported studies were confined to the sulfated titania and zirconia pillared systems. In particular, there is no report on the sulfate-supported tran-

* Corresponding author. Fax: +91 657 2270527.
E-mail address: drtmishra@yahoo.com (T. Mishra).

0021-9797/$ – see front matter
doi:10.1016/j.jcis.2006.05.013

sition metal mixed oxide pillared clay systems. Therefore, it seems to be interesting to study sulfate-supported mixed metal oxide pillared systems so as to understand the effect of sulfate on the physicochemical properties of mixed oxide pillared clay. In this context, the present paper deals with the characterization and catalytic activity of sulfate-supported iron–chromium mixed oxide pillared clay. Alcohol dehydration and aromatic alkylation reactions were used to understand the effect of sulfate on the catalytic behavior of the material.

2. Experimental

2.1. Material preparation

Sodium-exchanged montmorillonite of the Mainburg area, Germany, having an ion-exchange capacity of 85 meq/100 g and surface area of 85 m^2/g was used as the starting material for the pillared clay preparation. Aqueous solutions of trinuclear acetate complexes of iron(III) and chromium(III) were used as precursors. Both complexes were prepared according to the reported methods [16,17] and used as such. Pillared materials were prepared as per the general method given earlier [9]. In this experiment the total metal complex to clay ratio was maintained at 30 mmol/g instead of 20 mmol/g by varying the Fe(III) to Cr(III) ratio from 1/29 to 5/25. It was noted that the uptake of Fe(III) complex by the said clay is quite high in comparison to that of the Cr(III) complex. Therefore, it is necessary to maintain a minimum amount of Fe(III) in the mixed solution so as to prepare a sample having nearly the same amount of iron and chromium content. All five samples were filter-washed and dried at 100 °C for further use.

Sulfate-supported samples were prepared by the incipient wetness method using ammonium sulfate as the source and 100 °C dried pillared samples as precursor. Sulfate amount was varied from 1 to 5 wt% of the pillared clay sample. All the prepared samples were calcined at 300, 400, and 500 °C for further studies.

2.2. Estimation of iron and chromium in the samples

The amount of iron and chromium present in the material was estimated by AAS (Chemito-203) after acid dissolution.

2.3. XRD analysis

XRD patterns of the clay samples oriented on glass slides were recorded on a Philips semiautomatic diffractometer with Ni filter using Cu$K\alpha$ radiation from $2\theta = 2°$ to 20°. Basal spacing was calculated from the d_{001} value.

2.4. Surface area measurement

Surface area (BET) was determined by the nitrogen adsorption desorption method at liquid nitrogen temperature using a Quantasorb (Quantachrome, USA). Prior to the measurement, all the samples were degassed at 120 °C at 10^{-3} Torr for 5 h.

2.5. Ammonia TPD

Ammonia TPD was performed with the help of a CHEM BET-3000 (Quantachrome, USA) instrument in the temperature range of 30–800 °C. About 0.1 g of powdered sample was taken inside a quartz U tube and degassed at 350 °C for 1 h with ultrapure helium gas. After the sample was cooled to room temperature, NH_3 gas of 1000 ppm with N_2 gas was passed through the sample for 1 h. Then the ammonia adsorbed sample was purged with helium gas at 40 °C to remove any weakly adsorbed NH_3 on the surface. TPD was carried out at a heating rate of 10 °C/min to record the spectra.

2.6. Catalytic activity

Methanol dehydration of all the samples was performed in a fixed bed catalytic reactor (10 mm) with an on-line GC. Prior to the reaction study all the catalysts were preheated at 300 °C in a nitrogen atmosphere for 1 h. Methanol was quantitatively supplied to the reactor from a continuous microfeeder (Orion, USA) through a vaporizer using nitrogen as the carrier gas. All the connections from reactor to the GC were heated at 120 °C by a heating tape to avoid condensation of alcohol or the liquid products inside the apparatus. Reaction products were analyzed by means of an on-line GC (Sigma, India) in FID mode using a Porapaq Q column.

Alkylation of benzene and substituted benzenes with isopropanol was studied in a micropulse catalytic reactor (Sigma, India) with an on-line GC. Prior to the reaction, all the catalysts were preheated inside the reactor in a nitrogen atmosphere at 300 °C for 1 h. The volume of each pulse (mixture of benzene and isopropanol) was maintained at 1 μL. The catalytic reaction was studied using all the prepared sulfated materials varying the isopropanol to benzene ratio and temperature. Products were analyzed with the help of a 10 ft SS column with 10% TCEP.

3. Result and discussion

3.1. Intercalation

The uptake of chromium(III) and iron(III) complexes from their mixed aqueous solution by the sodium-exchanged montmorillonite is presented in Table 1. Similar to the earlier observation [9], the total complex uptake increases with the increasing Fe to Cr ratio in the solution. In all the cases the iron(III) uptake percentages from the solution is quite high in comparison to that of chromium(III) uptake which proves the higher affinity of the clay toward the iron(III) acetate complex. Earlier it was proposed that the high affinity might be due to the formation of polymeric species due to the slow partial hydrolysis of the iron(III) complex in aqueous solution. Therefore, here one sample was prepared using methanol as the solvent instead of water to avoid the hydrolysis to some extent. However, the uptake of iron(III) complex by the said clay remains nearly same. On the other hand iron(III) present in the clay layer may acts as a nucleation center where possible agglomeration takes place, thus increasing the iron uptake. Therefore it is difficult to give

Table 1
Variation in Cr(III) and Fe(III) uptake due to the variation in the iron to chromium ratio in the mixed complex aqueous solution

Samples	Fe/Cr in the solution[a]	Fe(III) in the clay (wt%)	Cr(III) in the clay (wt%)	Fe(III) intercalated (wt%)	Cr(III) intercalated (wt%)	Fe/Cr in the pillar	Fe/Cr in the material
1	1/29	4.1	0.02	4.86	8.82	0.551	1.016
2	2/28	4.1	0.02	7.16	6.75	1.061	1.668
3	3/27	4.1	0.02	8.84	5.22	1.693	2.479
4	4/26	4.1	0.02	9.77	4.47	2.186	3.103
5	5/25	4.1	0.02	10.38	3.98	2.608	3.638

[a] Iron to chromium ratio (Fe/Cr) is used as sample code.

Table 2
Basal spacing and surface area of prepared samples calcined at different temperatures

Sample code	SPCP[a]	Basal spacing (Å)			Surface area (m^2/g)	
		110 °C	300 °C	500 °C	300 °C	500 °C
1/29	–	21.8	18.0	17.7	230	276
2/28	–	21.9	18.0	17.8	234	278
3/27	–	22.0	18.1	17.8	236	279
4/26	–	22.3	18.3	17.9	236	281
5/25	–	22.4	18.4	17.9	239	284
2/28 + 1.0S	4.977	21.8	18.0	17.7	229	274
2/28 + 2.0S	9.954	21.9	18.1	17.8	228	269
2/28 + 3.0S	14.93	21.9	18.1	17.8	201	238
2/28 + 5.0S	24.885	21.9	18.1	17.8	152	178
5/25 + 2.0S	9.683	22.4	18.5	17.9	229	268

[a] SPCP indicates the sulfate wt% corresponding to oxide pillars only.

an exact reason for the higher uptake of the iron(III) complex in a mixed solution as both complexes have nearly the same molecular size.

It is well observed (Table 1) that with the increase in the total metal ion to clay ratio from 20 mmol/g [9] to 30 mmol/g, the complex uptake increases. Among all the prepared samples, 2/28 contains nearly equal amount of iron and chromium in the pillars as the ratio is 1.06. Therefore, for further study we have used this sample for sulfate impregnation. For comparison a 5/25 sample is also used. Ammonium sulfate is used as the source of sulfate ion to avoid the probability of destruction of pillars in the presence of strong acids like H_2SO_4. In the sample code sulfate is expressed as "S" with the amount added (wt%).

3.2. Textural properties

From the low-angle XRD it is observed that all the samples are stable up to 500 °C even after sulfate impregnation. Basal spacing is determined after calcinations at 300 °C or above as both complexes decompose at around 300 °C. A little difference in d_{001} basal spacing (Table 2) is observed due to the variation in Fe/Cr ratio. Basal spacing slightly increases with the increase in total metal ion uptake. Even after sulfate impregnation there is no change in the basal spacing in the sample. It seems that sulfate addition in low quantities through ammonium sulfate has no major effect toward the pillar structures as reported earlier [11]. However, there is a little decrease in the surface area due to the sulfate addition up to 2 wt% in the sample. Particularly, a substantial decrease in the surface area is noted when sulfate loading increases above 2 wt%.

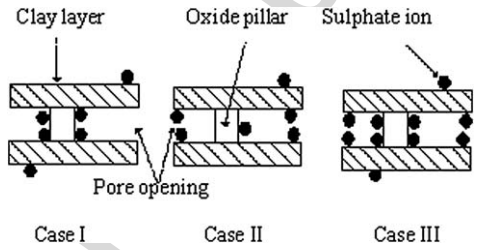

Fig. 1. Presentation of the proposed interaction of sulfate ion with the pillared clay.

Based on the surface area result, we would like to put forward an hypothesis (Fig. 1) on the type of interaction of the sulfate group with the pillared clay. Probably, sulfate preferentially goes to the pillars and hence a negligible decrease in the surface area for 1 and 2 wt% sulfated samples as shown in case I. After saturation of the pillar surfaces excess sulfate probably prefers the clay surface which may results in partial blockage of the pore opening as in case III. Hence the decreasing surface area is observed for a 3 wt% and above sulfate loading. Had there been a case II type of interaction in the first stage of sulfate addition (1–2 wt%), then an appreciable decrease in the surface area should have been observed. Again, had there been uniform dispersion of sulfate on the material surface then an appreciable decrease in the surface area should not have occurred at 3–5 wt% sulfate loading. However, taking into account the sulfate weight percentage corresponding to the oxide pillars only (SPCP) (Table 2) nearly 10 wt% of sulfate covers the pillars without decreasing the surface area. So also for sulfated metal oxide systems a decrease in the surface area and catalytic activity was reported [18] when sulfate loading increases above 10 wt%. Of course, the interaction of sulfate with the pillared clay may be more complex in the real system and at this stage we do not have enough proof to strengthen the proposed hypothesis.

3.3. Ammonia TPD

Generally, sulfate groups generate both strong Lewis and Brønsted acid sites when adsorbed to metal oxide surfaces. Sulfate species are itself Lewis acids or by attracting electrons, they generate Lewis acid centers on the oxide surfaces. The presence of these Lewis acid sites increases the Brønsted acid strength of the surface hydroxyl groups. The ammonia TPD is generally used [19] to characterize the acid site distribution and also to obtain the quantitative amount of acid sites in the temperature

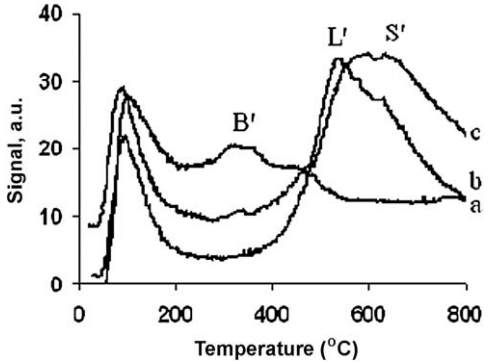

Fig. 2. Ammonia TPD curves of different samples calcined at 500 °C: (a) 2/28, (b) 2/28 + 1.0S, and (c) 2/28 + 2.0S.

range. In the TPD profile (Fig. 2) only two peaks were observed for the simple pillared clay (a). The initial peak (90–120 °C) which was observed in all three cases is due to the presence of weak acid sites. This peak more or less remains the same even after the sulfate addition. Peak (B′) observed within 300–350 °C is mostly due to the ammonia desorption from Brønsted acid sites [20,21]. Interestingly, due to the sulfate addition a new intense peak (L′) is observed within 450–600 °C, which may be corroborated with the presence of strong Lewis acid sites [20,21]. A similar observation was reported for sulfated zirconia [22] and titania–zirconia [20] systems. For a 2 wt% sulfate loading again a peak within 300–350 °C is observed which may be assigned to the NH_3 desorbed from Brønsted acid sites [20]. However, the peak due to the presence of Brønsted acid site is less intense for sulfated samples. It seems that strong Lewis acid sites are formed at the cost of some of the Brønsted acid sites due to the sulfate addition. In total the TPD profile of sulfated iron–chromium mixed oxide systems is quite comparable to that of sulfated metal oxide systems. For samples (b) and (c), another strong peak (S′) is observed at around 650 °C jointly with the L′ peak, which may be due to the decomposition of a sulfate group [20]. So the intensity of this peak also increases with the increasing sulfate content.

3.4. Methanol conversion

Usually methanol conversion over acidic catalysts gives three types of products: (a) C_2 or higher hydrocarbons, (b) dimethyl ether (DME), and (c) decomposition products of DME ($CO + CH_4$). Table 3 indicates an increase in the total conversion as well as C_{2+} hydrocarbon selectivity due to the sulfate addition up to 2 wt% at all temperatures which can be corroborated to the increasing number of acid sites. However, above 2 wt% sulfate there is a decrease in total conversion as well as the selectivity of C_{2+} hydrocarbons. Partial pore blocking due to the accumulation of sulfate on the surface, which restricts the available sites for the catalytic reaction may be the reason for the observed decrease in conversion and selectivity at higher sulfate contents. This again supports our proposed case III structure in Fig. 1 where accessibility of acid sites inside the pores is limited to some extent. Interestingly, the amount of chromium oxide and iron oxide present in the sample

Table 3
Methanol conversion at different temperatures on different samples

Temperature (°C)	Methanol conversion[a] (mol%)				
	2/28	2/28 + 1.0S	2/28 + 2.0S	2/28 + 3.0S	5/25 + 2.0S
300	11.4 (0.255)	14.5 (0.33)	16.7 (0.49)	13.6 (0.27)	16.5 (0.48)
350	26.5 (0.43)	36.4 (0.64)	45.5 (0.98)	34.0 (0.62)	45.0 (0.96)
400	47.8 (0.948)	62.5 (1.1)	74.0 (1.29)	60.5 (1.13)	73.4 (1.26)
450	77.5 (1.05)	84.5 (1.19)	95.4 (1.37)	81.6 (1.18)	94.6 (1.36)

[a] Numbers in the parentheses are the ratio of C_{2+} hydrocarbons to DME.

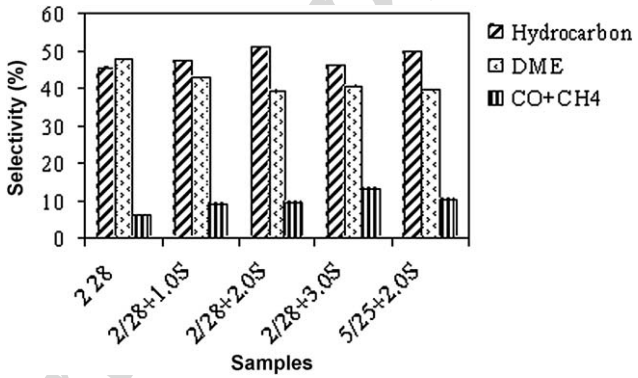

Fig. 3. Product selectivity of methanol conversion at 400 °C over different samples.

also plays some role for the hydrocarbon selectivity even after sulfate impregnation as observed for the 5/25 + 2.0S sample.

Out of the 2 wt% sulfated samples (2/28 and 5/25), 2/28 with a higher chromium content showed higher hydrocarbon selectivity. On the other hand decomposition product selectivity increases with the increase in iron oxide content in the samples (Fig. 3).

Again with the increase in the sulfate content the decomposition product selectivity also increases particularly at higher temperatures. This may be due to the presence of strong acid sites which bind the primary products after formation, thus creating the opportunity for the secondary reactions. It seems that the increasing sulfate content facilitates the secondary reaction, thus increasing the selectivity of both C_{2+} hydrocarbons and the decomposition products.

From the ammonia TPD it is clear that the sulfated samples mostly contain strong Lewis acid sites comparable to the other sulfated metal oxide systems. On the other hand, dehydration of methanol to hydrocarbons proceeds mostly on Brønsted acid sites [23]. So it is difficult to give an appropriate explanation for the remarkable increase in hydrocarbon selectivity for sulfated samples.

3.5. Alkylation of benzene

In the alkylation reaction only sulfated samples were used due to their better catalytic activity in the methanol conversion reaction. Gas-phase alkylation of benzene with isopropanol generally gives cumene and propene as major and 1,3-diisopropyl benzene and 1,4-diisopropyl benzene as minor products. In the cumene formation the benzene to isopropanol ratio also plays an important role. At low benzene

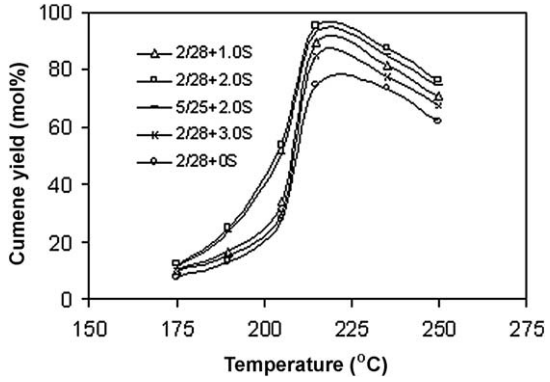

Fig. 4. Cumene formation from alkylation of benzene at different temperatures.

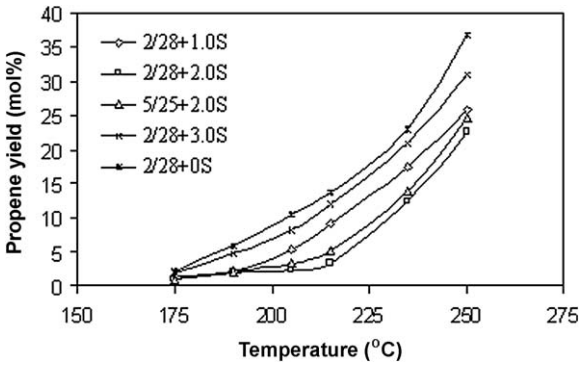

Fig. 5. Propene formation from alkylation of benzene at different reaction temperatures.

to isopropanol ratios propene selectivity is more even at low temperatures. In this study all the experiments were carried out with a benzene to isopropanol ratio of 12. It is observed that the cumene selectivity increases with the increase in temperature up to 215 °C and then decreases (Fig. 4). However, the propene formation is low up to 215 °C and then suddenly increases with increasing reaction temperature (Fig. 5). So it appears that at higher temperatures isopropanol mostly dehydrates directly to propene without further interaction with benzene, thus decreasing the cumene selectivity.

Formation (<2 mol%) of 1,3-diisopropyl benzene is noted within the temperature range of 190–210 °C for the sulfated samples. However, formation of 1,4-diisopropyl benzene is negligible. Above all, there is a substantial increase in the isopropylation activity due to the sulfate loading which may be corroborated with the increasing numbers of acid sites.

It is well known that the alkylation of benzene with isopropanol/propene is an acid-catalyzed reaction and mostly takes place on the Brønsted acid sites of zeolites [24]. However, from the ammonia TPD it is evident that the sulfated material mostly contains strong Lewis acid sites and few Brønsted acid sites. Therefore, similar to that of methanol dehydration again there is a need to explain the increase in the cumene formation for sulfated catalysts. In the reaction mechanism the first step involves the dehydration of isopropanol to propene and water. The dissociative adsorption of generated water from the dehydration process could transform the available strong Lewis acid sites to Brønsted sites. In fact, this type of transformation

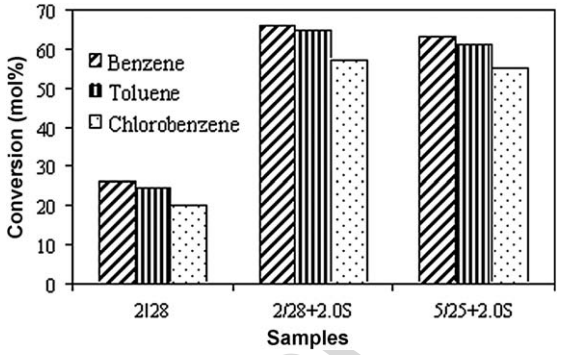

Fig. 6. Isopropylation of substituted benzenes over sulfated materials at 215 °C.

was reported for alcohol dehydration on ZrO_2–TiO_2 and ZrO_2–Al_2O_3 mixed oxides [19] and tungstated ZrO_2 [25]. Probably this is the reason for the higher conversion and hydrocarbon selectivity in the methanol dehydration reaction also.

The same catalysts are also used for the alkylation of a series of substituted benzene with isopropanol at 215 °C. From Fig. 6 it is observed that the isopropylation of benzene and chlorobenzene is highest and lowest, respectively. However, the alkylation of toluene is expected to be more favorable than benzene due to the electron-releasing nature of the methyl group [26]. On the contrary, the yield of alkylated product is slightly higher for benzene which is difficult to explain at this stage. Diffusion of toluene inside the pores may be slow in comparison to that of benzene due to the difference in their molecular size and hence the decrease in the yield. Higher paraselectivity is noted for both toluene and chlorobenzene alkylation. This may be due to the steric factor of the pores of the catalysts which prohibits the ortho substitution. This type of high paraselectivity was also noted for the nitration of substituted benzenes on pillared clay [27]. In total, 2 wt% sulfate loaded samples show the highest alkylation activity and hence can be better utilized as solid alkylation catalysts. In particular, the 2/28 + 2.0S sample exhibits better catalytic activity than the 5/25 + 2.0S sample.

4. Conclusion

Stable sulfate-supported iron–chromium mixed oxide pillared clay with enhanced catalytic activity can be prepared by the aqueous impregnation method using ammonium sulfate as the source. Prepared materials were found to be stable up to 500 °C having a basal spacing of ⩾17.7 Å. A little decrease in the surface area was observed due to sulfate loading up to 2 wt%. However, sulfate loading above 2 wt% significantly decreases the surface area as well as catalytic activity which may be due to the pore blocking by sulfate species. The formation strong Lewis acid sites at the cost of some of the Brønsted acid sites was evident from the ammonia TPD profile of sulfated samples. Irrespective of reaction temperature C_{2+} hydrocarbon and decomposition product selectivity increase due to the sulfate loading. Among all the prepared materials, 2/28 + 2.0S sample was found to be a better catalyst for alcohol dehydration and aromatic alkylation reactions. Improved catalytic activity may be due to the increase in available acid sites with the sulfate loading. From the above study it can be concluded that low

sulfate loading (up to 2 wt%) can enhance the surface acidity of the pillared clay, thus making it a better acid catalyst.

Acknowledgments

The authors are thankful to Prof. S.P. Mehrotra, Director, National Metallurgical Laboratory, Jamshedpur, for his constant encouragement and permission to publish this paper and to Dr. S.K. Tiwari for his cooperation throughout this work. One of the authors (T.M.) is thankful to DST, New Delhi, India, for providing financial help for this work.

References

[1] I.V. Mitchel (Ed.), Pillared Layered Structures: Current Trends and Applications, Elsevier, London, 1990.
[2] R. Burch, Catalysis Today, Pillared Clays, Elsevier, Amsterdam, 1988.
[3] T. Mishra, K.M. Parida, Appl. Catal. A 166 (1998) 123.
[4] F. Bergaya, N. Hassoum, L. Gatineau, J. Barrault, in: Preparation of Catalyst, vol. V, Elsevier, Amsterdam, 1991, p. 329.
[5] W.Y. Lee, R.H. Raytha, B.J. Tatarchun, J. Catal. 115 (1989) 159.
[6] J. Sterte, in: Preparation of Catalyst, vol. V, Elsevier, Amsterdam, 1991, p. 301.
[7] S.A. Bagshaw, R.P. Cooney, Chem. Mater. 7 (1995) 1384.
[8] S.P. Skaribas, P.J. Pomonis, P. Grange, B. Delmon, J. Chem. Soc. Faraday Trans. 88 (1992) 3217.
[9] T. Mishra, K.M. Parida, Appl. Catal. A 174 (1998) 91.
[10] S. Ben Chaabene, L. Bergaoui, A. Ghorbel, J.-F. Lambert, Stud. Surf. Sci. Catal. 143 (2002) 1053.
[11] M. Katoh, H. Fujisawa, T. Yamaguchi, Stud. Surf. Sci. Catal. 90 (1994) 263.
[12] L. Khalfallah Boudali, A. Ghorbel, D. Tichit, F. Figueras, R. Dutartre, Microporous Mater. 2 (1994) 525.
[13] J.F. Knifton, US Patent 5352847 (1993).
[14] S. Benchaabene, L. Bergaoui, A. Ghorbel, J.F. Lambert, P. Grange, Appl. Catal. A 252 (2003) 411.
[15] A.S.C. Brown, J.S.J. Hargreaves, S.H. Taylor, Catal. Today 59 (2000) 403.
[16] S. Yamanaka, D. Tadahiro, S. Sako, M. Hattori, Mater. Res. Bull. 19 (1984) 161.
[17] C. Oldham, Prog. Inorg. Chem. 10 (1968) 223.
[18] H.K. Mishra, K.M. Parida, Appl. Catal. A 224 (2002) 179.
[19] C. Lahousse, A. Aboulayt, F. Mauge, J. Bachelier, J.C. Lavalley, J. Mol. Catal. 84 (1993) 283.
[20] R. Barthos, F. Lonyi, G.Y. Onyestyak, J. Valyon, J. Phys. Chem. B 104 (2000) 7311.
[21] R. Barthos, F. Lonyi, G.Y. Onyestyak, J. Valyon, Solid State Ionics 141/142 (2001) 253.
[22] H. Suja, C.S. Deepa, K. Sreeja Rani, S. Sugunan, Appl. Catal. A 230 (2002) 233.
[23] H. Pines, The Chemistry of Catalytic Hydrocarbon Conversion, Academic Press, New York, 1981.
[24] A. Corma, V.M. Soria, E. Schoeveld, J. Catal. 192 (2000) 163.
[25] C.D. Baertsch, K.T. Komala, Y.-H. Chua, E. Iglesia, J. Catal. 205 (2000) 44.
[26] J.J. McKetta (Ed.), Chemical Processing Handbook, Dekker, New York, 1993, p. 763.
[27] T. Mishra, K.M. Parida, J. Mol. Catal. A 121 (1997) 91.